Journal of Renewable Materials

Tech Science Press

DOI: 10.32604/jrm.2022.019548

ARTICLE

Phosphorylated Salicylic Acid as Flame Retardant in Epoxy Resins and Composites

Lara Greiner[1,*], Philipp Kukla[2], Sebastian Eibl[1] and Manfred Döring[3]

[1]Bundeswehr Research Institute for Materials, Fuels and Lubricants, Erding, 85435, Germany

[2]Fraunhofer Institute for Structural Durability and System Reliability LBF, Darmstadt, 64289, Germany

[3]Schill+Seilacher GmbH, Böblingen, 71032, Germany

[*]Corresponding Author: Lara Greiner. Email: laragreiner@bundeswehr.org

Received: 29 September 2021 Accepted: 01 December 2021

ABSTRACT

A novel, versatile flame retardant substructure based on phosphorylated salicylic acid (SCP) is described and used in the synthesis of new flame retardants for HexFlow® RTM6, a high-performance epoxy resin used in resin transfer molding processes as composite matrix. The starting material salicylic acid can be obtained from natural sources. SCP as reactive phosphorus chloride is converted with a novolak, a novolak containing 9, 10-dihydro-9-oxa-10-phospha-phenanthrene-10-oxide (DOPO) substituents or DOPO-hydroquinone to flame retardants with sufficient thermal stability and high char yield. Additionally, these flame retardants are soluble in the resin as well as react into the epoxy network. The determined thermal stability and glass transition temperatures of flame retarded neat resin samples as well as the interlaminar shear strength of corresponding carbon fiber reinforced composite materials showed the applicability of these flame retardants. Neat resin samples and composites were tested for their flammability by UL94 and/or flame-retardant performance by cone calorimetry. All tested flame retardants decrease the peak of heat release rate by up to 54% for neat resin samples. A combination of DOPO and SCP in one flame retardant shows synergistic effects in char formation and the mode of action adapts to neat resin or fiber-reinforced samples, so there is efficient flame retardancy in both cases. Therefore, a tailoring of SCP based flame retardants is possible. Additionally, these flame retardants efficiently reduce fiber degradation during combustion of carbon fiber-reinforced epoxy resins as observed by scanning electron microscopy and energy dispersive X-ray spectroscopy.

KEYWORDS

Epoxy resin; composite; fiber protection; bio-based; flame retardant

1 Introduction

High performance epoxy resins are used in a variety of applications. To improve their mechanical properties, carbon fibers are often used as reinforcement, for example in aerospace engineering. These sophisticated applications require efficient flame retardancy while mechanical and thermal properties as well as chemical resistance and low shrinkage should be maintained. Current research not only focuses on polymeric, reactive, phosphorus containing flame retardants in terms of no leaching, good material properties and low toxicity but also on green solutions. The efficiency of incorporated flame retardants

depends on the epoxy matrix and the reinforcement [1–10]. For phosphorus containing flame retardants, the mode of action is not only dependent on matrix, additives, and reinforcement, but also on the chemical environment of the phosphorus [11,12]. If the chemical environment of the phosphorus is carbon/hydrogen rich, it promotes action in the gas phase. An oxygen rich environment promotes action in the condensed phase, respectively. Different phosphorus species may also act synergistic [13].

Literature focuses on different approaches in bio-based flame retardants. These can be made partially or totally from renewable resources. For example, basic compounds like benzaldehyde [14], pentaerythritol [15,16], phytic acid [17–19] or tartaric acid [20] may be gained from renewable resources and used to synthesize flame retardants. A widely used method is phosphorylation of bio based molecules or to chemically bond common phosphorus containing compounds to biobased, organic structures like lignin [21,22], acrolein [23], tartaric acid [24], itaconic acid [25], eugenol [26], cardanol [26], benzaldehyde [27,28], vanillin [29] or starch-derived structures like isosorbide [30] and bis-2,5-(hydroxymethyl) furan [31]. Common phosphorus containing reagents are 9,10-dihydro-9-oxa-10-phospha-phenanthrene-10-oxide (DOPO) derivatives, phenylphosphoric dichloride, dichlorophenylphosphate, diphenylphosphate chloride, diphenylphosphoric chloride, dimethylphosphite or 5,5-dimethyl-[1,3,2] dioxaphosphinane-2-oxide (DDPO) etc. Non-reactive flame retardants are used in epoxy resins [32–36] as well as flame retardants that are incorporated to the network [37–42] for example as hardener [43] or epoxy component [44,45]. In general, there are many possibilities to combine phosphorus derivatives like DOPO or other mentioned compounds, but the literature lacks bio based, low-molecular, versatile, reactive phosphorus containing substructures with efficient flame retardancy.

Therefore, this paper addresses a structure that has not yet been used as flame retardant reactant: 2-chloro-1,3,2-benzodioxaphosphorin-4-one (SCP, Fig. 1). This compound can be synthesized by reaction of salicylic acid and phosphorus trichloride [46,47]. Salicylic acid is a renewable raw material which can be extracted from meadow bark or isolated from meadowsweet [48,49]. SCP has a high potential as flame retardant precursor since it has an aromatic substructure and a high oxygen content promoting action in the condensed phase by char formation. Furthermore, it is a phosphorus chloride and can act as a possible precursor for versatile reactions, so that processability, thermal stability, the properties of resin formulations as well as flame retardant efficiency and mode of action can be adjusted. In this work, due to the low thermal stability of SCP itself, novolak and DOPO-Hydroquinone (DOPO-HQ, Fig. 2) were used to synthesize adjusted flame retardants. Both reactants have multiple hydroxyl groups that may react to the epoxy network for example to prevent leaching. Furthermore, novolak is a polymeric structure which is promising in terms of thermal and mechanical properties as well as processing [2,50–56]. DOPO-HQ was chosen to add another phosphorus species with a different chemical environment. A possible synergism of different phosphorus species is the reason, why in a third approach, SCP and DOPO were bonded to a novolak structure. The flame retardants were tested in the high-performance epoxy resin RTM6® as well as in carbon-fiber reinforced composites thereof. As mentioned above, the flame retardant efficiency is also dependent on the matrix. For RTM6, different combinations with DOPO-containing flame retardants are published, but not focusing on renewable materials. For example, Perret et al. [2] tested star-shaped DOPO-containing flame retardants and reached V0 classification in UL94 vertical burning tests for 2% phosphorus in neat RTM6 samples (thickness 3 mm). Neat non-flame retarded RTM6 reaches no classification. Latest studies [54] concerning DOPO-containing polyacrylamides showed V0 classifications in UL94 vertical burning tests with 0.9% phosphorus in neat RTM6 samples (thickness 4 mm).

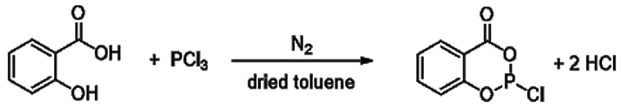

Figure 1: Reaction of salicylic acid to SCP

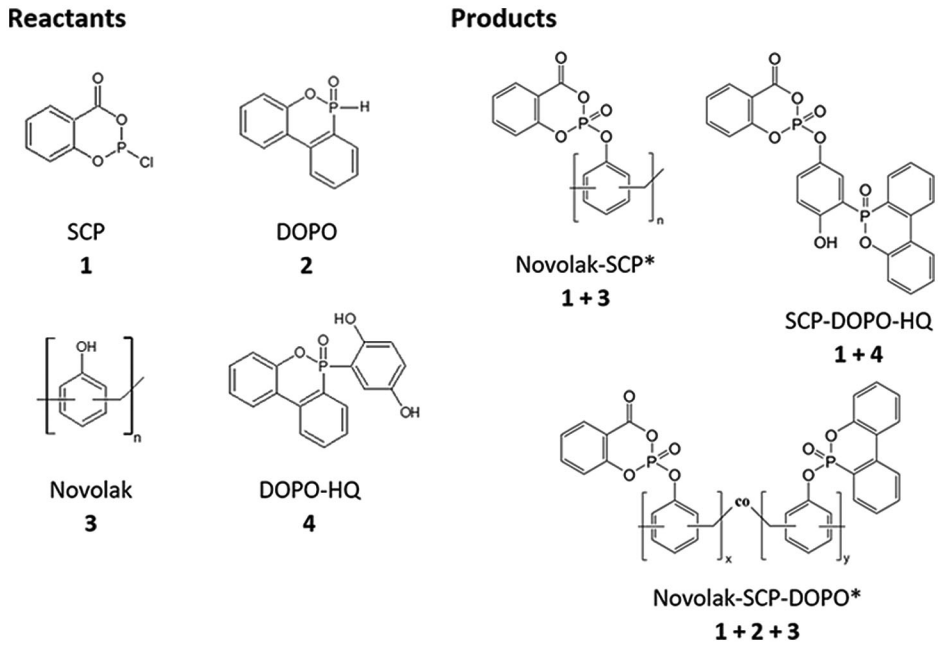

Figure 2: Chemical structures of the reactants novolak, DOPO-HQ, SCP and DOPO as well as schematic structures of the products Novolak-SCP, SCP-DOPO-HQ and novolak-SCP-DOPO. ***Contain at least 67% residual OH-moieties**

While the epoxy resin matrix shows hazards like smoke, heat and toxic gases during combustion, the incorporation of carbon fibers leads to an additional hazard. It is well known that carbon fibers can form respirable fiber fragments after a thermal load and fire [57,58]. For example, critical fiber concentrations were reported for large-scale fire tests and for collecting the flight recorder of a crashed helicopter [59,60]. Within minutes, a significant oxidation reaction is observed above 650°C in air [57]. According to the definition of the World Health Organization (WHO), fibers thinner than 3 µm longer than 5 µm are respirable. Additionally, the length to diameter ratio must be higher than 3. Fibers with these dimensions are thin enough to penetrate the deep lung areas (alveoli), and too long to be exhaled [61]. Commercially available carbon fibers are typically thicker than 5 µm and, therefore, uncritical regarding inhalation. Since this paper focuses on a high-performance epoxy resin used in aircraft construction, a possible fiber protection gained by the synthesized flame retardants is investigated as well. While a mode of action in the gas phase seems promising for fiber reinforced composite materials due to a high surface of the matrix in the composite, a condensed phase activity seems necessary to protect the fibers since a protection layer has to be formed during combustion. Latest results [54,62] showed a promising fiber protection by incorporation of char-forming or intumescent phosphorus-containing flame retardants to the matrix. In contrast to zinc borate, that has already been proposed as well [57], these flame retardants are soluble in the epoxy resin matrix and typical injection processes that are used for the production of fiber reinforced materials are possible. Therefore, this research focuses on a new approach to use renewable sources for efficient fiber protection and flame retardancy, while maintaining the excellent high

performance epoxy resin properties as well as the processability of the resin formulation by application of SCP as novel flame retardant reactant.

2 Experimental

2.1 Materials

Unless stated otherwise, solvents and chemicals were obtained from commercial sources and used as received: acetonitrile (99.9% Acros Organics, Belgium), carbon tetrachloride (CCl_4, 99.8%, Sigma Aldrich, Germany), chloroform (99.9%, Acros Organics, Belgium), DOPO (95%, Schill+Seilacher GmbH), DOPO-HQ (95%, Schill+Seilacher GmbH), phosphorus trichloride (99%, Acros Organics, Belgium), salicylic acid (98%, VWR Chemicals, USA), triethylamine (TEA, 99.5%, VWR Chemicals, USA). The novolak used was Bakelite® PF 0205 DF 04 ($M_w = 878\ g{\cdot}mol^{-1}$, 0.12% moisture content, Bakelite, Germany). All syntheses were carried out under nitrogen atmosphere and with dry equipment.

Chemical structures of the synthesized flame retardants are shown in Fig. 2.

2.2 Synthesis of 2-Chloro-4-oxo-5, 6-Benzo-1,3,2-Dioxaphosphorinane (SCP)

In a dry three-neck flask 150 g salicylic acid (1.086 mol, 1.0 eq) and 145 mL phosphorus trichloride (1.658 mol, 1.53 eq) were dispersed under reflux for 10 h. The pale-yellow liquid was distilled in vacuo to give a yellow liquid that crystallizes slowly to a white solid. The yield was 223.49 g (98.4%).

^{1}H-NMR (300 MHz, $CDCl_3$, 298 K) δ = 8.03 (dd, J = 7.9, 1.8, 1H), 7.64 (m, 1H), 7.43–7.20 (m, 1H), 7.20–6.97 (m, 1H) ppm.

^{31}P NMR (122 MHz, $CDCl_3$, 298 K): 148.02(s) ppm.

P-content (calculated): 15%.

2.3 Addition of SCP to Novolak (Novolak-SCP)

SCP (40.50 g, 200 mmol, 1.0 eq) and the novolak (65.00 g, about 600 mmol hydroxyl groups, 3.0 eq) were solved in 300 mL acetonitrile (dry) and within 3 h, triethylamine (TEA, 40 mL, 290 mmol, 1.4 eq) was added to the solution. A yellow precipitate was filtered, washed with water and dried in vacuo, yielding 94.55 g of product (96.4%). NMR results showed that autoxidation of the phosphorus occurred.

^{1}H NMR (300 MHz, DMSO-d6, 298 K) 8.12–7.48 (m, 3H), 7.09–6.49 (m, 36H), 4.01–3.44 (m, 12H).

^{31}P NMR (122 MHz, DMSO-d6, 298 K) 1.51 (s).

P-content (calculated): 8% | residual OH-groups: 67 mol%.

2.4 Atherton-Todd-Reaction of Novolak and DOPO + Addition of SCP (Novolak-SCP-DOPO)

In a dry three-neck flask at 0°C 85 g Novolak (about 800 mmol hydroxyl groups, 6 eq) was solved in 300 mL dry acetonitrile. Via a dropping funnel, a solution of DOPO (29 g, 134 mmol, 1.0 eq), TEA (22.0 mL 160 mmol, 1.2 eq) and CCl_4 (12.5 mL, 130 mmol, 1.0 eq) was added within 30 min. After 24 h at room temperature, the precipitate was filtered and washed. The intermediate product yield was 101.38 g (90.0%). SCP (26.58 g, 131 mmol, 1.0 eq) and the intermediate product were solved in 300 mL acetonitrile and within 3 h, TEA (15 mL, 160 mmol, 1.2 eq) was added to the solution. The yellow precipitate was filtered, washed with chloroform, and dried in vacuo, yielding 119.72 g of product (84.1%). NMR results showed that autoxidation of the phosphorus contained in SCP occurred.

^{1}H NMR (300 MHz, DMSO-d6, 298 K) 8.41–7.15 (m, 12H), 7.06–6.50 (m, 64H), 3.93–3.32 (m, 30H).

^{31}P NMR (122 MHz, DMSO-d6, 298 K): 6.19 (s, 51%), 1.26 (s, 49%).

P-content (calculated): 6% | residual OH-groups: 67 mol%.

2.5 Addition of SCP to DOPO-HQ (SCP-DOPO-HQ)

In a dry flask 24.03 g SCP (118 mmol, 1.0 eq)) and 38.37 g DOPO-HQ (118 mmol, 1 eq) were suspended in 250 mL chloroform (dry) and within 1 h, TEA (40 mL, 290 mmol, 1.4 eq) was added. After 4 h a homogeneous solution was formed, and the solvent was removed in vacuo. The product was washed with distilled water and dried, yielding 31.41 g (40.68%) of a white powder. NMR results showed that autoxidation of the phosphorus contained in SCP occurred.

^{1}H NMR (300 MHz, DMSO-d6, 298 K): 8.32–8.19 (m, 2H), 7.85–7.68 (m, 3H), 7.66–7.39 (m, 5H), 7.37–7.13 (m, 2H), 7.00–6.85 (m, 2H), 6.66 (dd, J = 8.8, 7.4, 1H).

^{31}P NMR (122 MHz, DMSO-d6, 298 K): 22.09 (s, 52%), 1.22 (s, 48%).

P-content (calculated): 12%.

Previous experiments showed that only monosubstitution of DOPO-HQ occurs and that there are 50% residual OH-groups.

Synthesized flame retardants were added to the epoxy based resin HexFlow® RTM6 in various portions of up to 15% and mixed at 120°C for 15 min. RTM6 mainly consists of tetraglycidyl methylene dianiline (TGMDA) and aromatic aminic hardeners. Carbon fiber reinforcement is introduced by the fabric HexForce® G0939, also provided by Hexcel Composites GmbH (Stade, Germany) [63]. 2 mm thick CFRP samples with $[(0|90)]_8$ lay-ups were prepared by modified hand lamination and curing in an autoclave according to literature [54,63]. A water-cooled diamond wheel saw was used to cut specimens for cone calorimetry: 100 mm × 100 mm and testing of interlaminar shear strength: 20 mm × 10 mm. Additionally, 2 and 4 mm thick resin samples without fiber reinforcement were cured with the same temperature program but under atmospheric pressure. Specimens of about 2 mm × 2 mm × 1 mm for differential scanning calorimetry and of 70 mm × 13 mm × 4 mm for UL94-tests were trimmed with a band saw. An overview of the prepared samples is given in Table 1.

Table 1: Samples prepared based on RTM6 resin

Flame retardant in RTM6-matrix	Reinforcement	Thickness/mm
-	-	4
7.5% Novolak-SCP	-	4
10% Novolak-SCP	-	4
15% Novolak-SCP	-	4
7.5% Novolak-SCP-DOPO	-	4
10% Novolak-SCP-DOPO	-	4
15% Novolak-SCP-DOPO	-	4
7.5% SCP-DOPO-HQ	-	4
10% SCP-DOPO-HQ	-	4
15% SCP-DOPO-HQ	-	4
-	*CF*	2
10% Novolak-SCP	*CF*	2
10% Novolak-SCP-DOPO	*CF*	2
10% SCP-DOPO-HQ	*CF*	2

CF: Carbon fiber

2.6 Characterization

^{1}H-and ^{31}P-Nuclear Magnetic Resonance (NMR, Nanobay 300, Bruker Corporation, Billerica, MA, USA) spectroscopy measurements were done at 300 MHz with 16 scans. Samples were dissolved in DMSO-d6 (deuterated dimethyl sulfoxide) or $CDCl_3$ beforehand and signals were referred to the solvent signal. Direct inlet-probe mass spectrometry (DIP-MS) was done with an Agilent 5975 MSD mass spectrometer (Agilent Technologies, Inc., US). The temperature program used started at 30°C, heated to 150°C (heating rate 0.3 $K{\cdot}s^{-1}$), stayed isothermal for 1 min, heated to 250°C, stayed isothermal for 1 min and finally heated up to 350°C. Thermogravimetric analyses (TGA; Q500, TA Instruments, Inc., USA) of flame retardants and the compact material were performed starting at room temperature and heated to 800°C in nitrogen or synthetic air (50 $ml{\cdot}min^{-1}$) with a heating rate of 10 $K{\cdot}min^{-1}$. Differential Scanning Analysis (DSC, DSC 822e, Mettler Toledo, Columbus, OH, USA) of neat resin samples or flame retardant mixtures with TGMDA was carried out from room temperature to 250°C with 10 $K{\cdot}min^{-1}$ in nitrogen atmosphere. Moisture absorption of neat resin samples was determined for at least two specimens. These samples were placed into different water-filled, closed beakers and heated inside an oven to 70°C. Their mass after 14 d is compared relatively to their initial mass. UL-94 vertical burning tests of 4 mm thick neat resin samples were carried out according to DIN EN 60695-11-10 [64] in a UL-94 test chamber (Dr.-Ing. Georg Wazau Mess-+ Prüfsysteme GmbH, Germany). Fiber-reinforced specimens and neat resin samples were tested for the determination of reaction-to-fire characteristics such as heat release, mass loss, formation of smoke, etc. [65] according to ISO 5660 [66] in non-scrubbed mode by cone calorimetric measurements (Fire Testing Technology Ltd., England). Specimens (100 × 100 mm^2) were wrapped in aluminum foil at the backside, supported on mineral wool, inserted in a frame sample holder, and irradiated. A heat flux of 60 $kW{\cdot}m^{-2}$ is used for reinforced samples and corresponds more to fully developed fires and additionally it is used to observe the fiber degradation. A heat flux of 35 $kW{\cdot}m^{-2}$ is used for neat resin samples and corresponds to developing fires [67]. A scanning electron microscope (SM-300, TOPCON Corp.) was used for the determination of fiber diameters. For each given value, the diameters of at least 30 fibers are averaged. EDX analyses were done on an EVO HD 25 (Carl Zeiss Microscopy GmbH, 5 kV) scanning electron microscope. Interlaminar shear strength (ILSS) tests were performed for 2 mm thick specimens in accordance with EN 2563 by a three-point flexural test with a universal mechanical testing machine (Z020, ZwickRoell GmbH & Co. KG, Germany) [68].

3 Results and Discussion

3.1 Characterization of SCP Based Flame Retardants

3.1.1 Thermal Stability and Degradation Products

The thermal stability of SCP itself is very low, which is expected, as it consists of a phosphorus chloride and is still very reactive. Important values of TG measurements (Fig. 3) in nitrogen or synthetic air are summarized in Table 2. The temperature at maximum mass loss rate (T_{max}), the initial degradation temperatures ($T_{1\%}$, $T_{5\%}$) at which 1% or 5% mass loss are reached and the residue at 800°C are shown. While degradation starts at low temperatures of about 40°C, the residues are high with 30% in nitrogen and 14% in air at 800°C. These high residues are a hint for a possible mode of action in the condensed phase for SCP containing structures. This is very promising in terms of flame retardant efficiency in neat resin samples with low surface of the combustible material as well as for the formation of a protective layer on carbon fibers during combustion, that is especially required at temperature loads over 650°C. Fig. 3 also shows TG measurements for Novolak and DOPO-HQ that were chosen to react with SCP to form stable flame retardants. The overall thermal stability of these compounds is higher than for SCP. Therefore, a combination of novolak or DOPO-HQ with SCP is a promising approach for the synthesis of flame retardants.

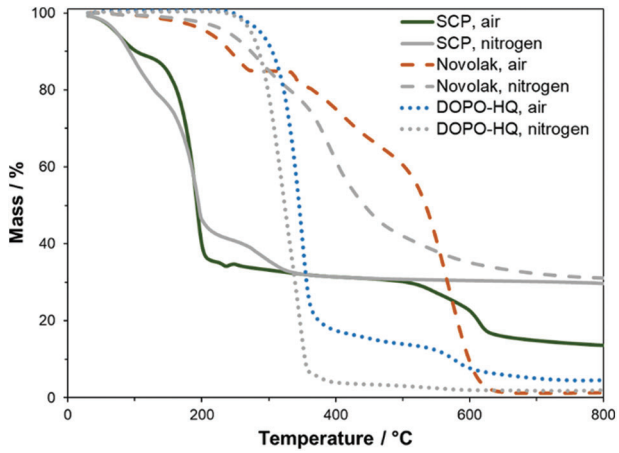

Figure 3: TG-curves of SCP, novolak and DOPO-HQ measured in nitrogen atmosphere and synthetic air

Table 2: T_{max}, $T_{1\%}$, $T_{5\%}$ and residue at 800°C of SCP based flame retardants obtained by TG measurements in air or nitrogen flow (50 mL·min^{-1}) with a heating rate of 10 K·min^{-1}

Sample	P-content/%	T_{max}/°C	$T_{1\%}$/°C	$T_{5\%}$/°C	Residue (800°C)/%
SCP, N_2	15	197	39	73	30
Novolak-SCP, N_2	8	490	128	183	26
Novolak-SCP-DOPO, N_2	6	519	108	183	34
SCP-DOPO-HQ, N_2	12	235	90	153	17
SCP, air	15	194	38	72	14
Novolak-SCP, air	8	480	126	188	2
Novolak-SCP-DOPO, air	6	481	86	175	0
SCP-DOPO-HQ, air	12	231	87	161	3

The thermal stability of the synthesized flame retardants was also determined by TG analysis. Important values are summarized in Table 2. Additionally, the calculated phosphorus content of the flame retardants is given. Fig. 4 shows the curves obtained from measurements in nitrogen atmosphere on the left side. There are at least two degradation steps observed. In nitrogen atmosphere, novolak containing species show similar initial degradation temperatures $T_{5\%}$ with 183°C. The degradation of SCP-DOPO-HQ starts at lower temperatures with a $T_{5\%}$ of 153°C. This shows that the initial decomposition temperature is increased using a novolak in combination with SCP. According to literature [69], DOPO-HQ starts to decompose at 359°C ($T_{5\%}$). This means that the addition of SCP lowers the decomposition temperature, and the two decomposition steps can be tentatively assigned to the decomposition of SCP components (T_{max} 235°C) and DOPO components (T_{max} 420°C). This corresponds to the multiple decomposition steps for Novolak-SCP-DOPO. The final decomposition of novolak units occurs in the last step (T_{max} 519°C). In general, novolak containing samples show higher residues. Especially the mixed species Novolak-SCP-DOPO, that has the lowest phosphorus content of 6%, has a very high residue of 34%. Novolak-SCP instead has a residue of only 26% with a primary phosphorus content of 8%. The molar ratio of phosphorus containing substituents to novolak monomers is the same for both compounds. Therefore, the replacement of half SCP units with DOPO units from Novolak-SCP to Novolak-SCP-DOPO has a huge impact on the

remaining residue. In conclusion, for Novolak-SCP-DOPO, the phosphorus species SCP and DOPO show a synergism in char formation. Up to 500°C the decomposition in air is like the decomposition in nitrogen atmosphere. The corresponding curves are shown in Fig. 4 on the right hand side. This means that the presence of oxygen has no apparent influence on the decomposition. At temperatures over 500°C, the decomposition of the formed char leads to residues of about 0% for all species. This decomposition refers to total oxidation as proven by FTIR spectra of evolving gases, only showing carbon dioxide.

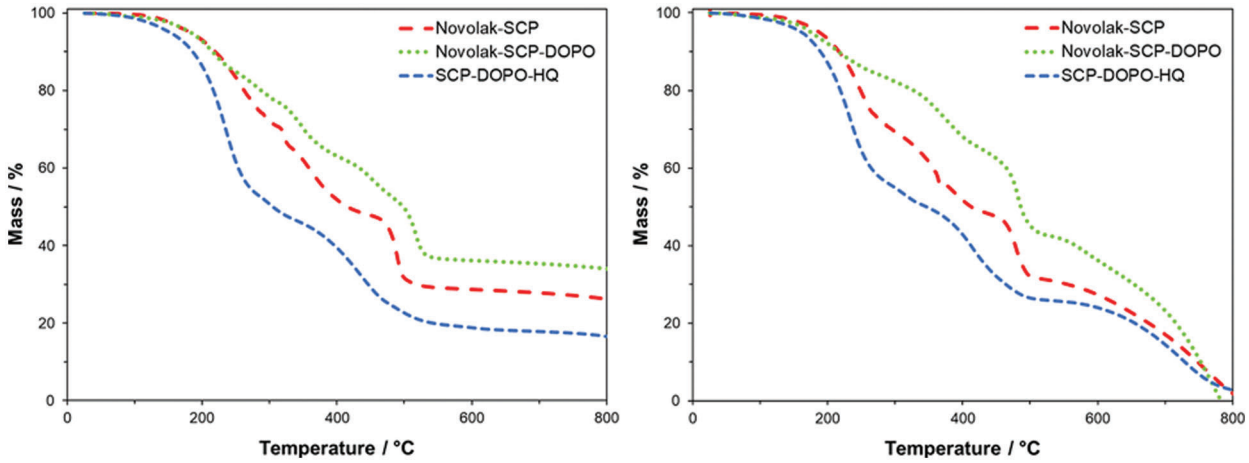

Figure 4: TG-curves of SCP-based flame retardants measured in nitrogen atmosphere (left) and synthetic air (right)

For further analysis and hints on decomposition and flame retardant properties, DIP-MS measurements were carried out. Possible structures of detected main fragments are shown in Fig. 5. SCP containing structures Novolak-SCP, Novolak-SCP-DOPO and SCP-DOPO HQ show derivatives of phosphoric acid (Fig. 5B) promoting a possible mode of action in the condensed phase, while DOPO-containing samples show the formation of typical DOPO-H fragments (Fig. 5C) promoting a mode of action in the gas phase.

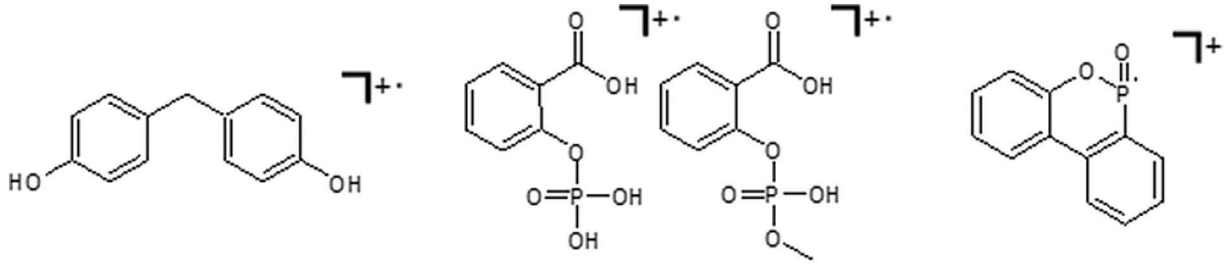

Figure 5: Possible structures of the main fragments detected by DIP-MS for novolak containing samples (A), SCP-containing samples (B) and DOPO-containing samples (C)

3.1.2 Reaction with Epoxy Compounds

Both, novolak compounds as well as SCP-DOPO-HQ contain residual hydroxyl groups. These functional groups may react with the epoxy component TGMDA (Fig. 6) during the network formation in the epoxy resin matrix. DSC measurements shown in Fig. 6 are used to observe a possible reaction. For all mixtures of flame retardants and TGMDA, exothermal reactions in the temperature range of

RTM6 processing up to 180°C can be observed. In comparable measurements of pure flame retardants or pure TGMDA, no exothermal processes have been detected. Therefore, the residual hydroxyl groups are likely to be incorporated into the epoxy network preventing for example leaching processes.

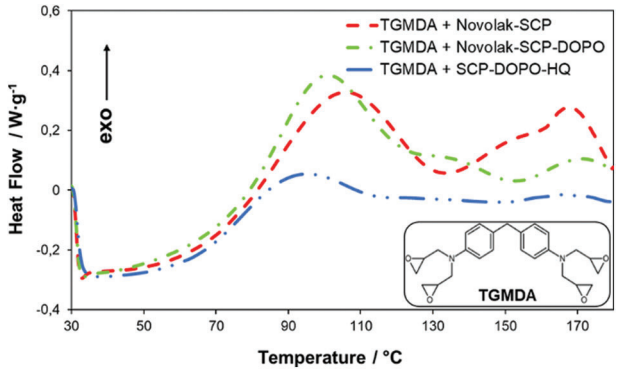

Figure 6: DSC curves of samples containing a flame retardant and TGMDA (heating rate 10 K·min^{-1}, nitrogen atmosphere)

3.2 Neat Resin Samples and Carbon Fiber Reinforced Composites

3.2.1 Glass Transition Temperature, Moisture Uptake and Interlaminar Shear Strength

Glass transition temperatures (T_g) were determined by DSC and are summarized in Table 3. The addition of 10% flame retardant to RTM6 epoxy resin leads to a decrease of 20 to 25°C for novolak containing compounds. This is caused by the reaction of phenol groups with the epoxy resin leading to a widening of the network and a deviation of stoichiometry between epoxy groups and amine groups of the hardening agent. However, this decrease in glass transition temperature is acceptable according to literature [2,54]. In contrast, SCP-DOPO-HQ leads to a decrease of the T_g by 40°C, which corresponds to a pronounced softening effect. Novolak containing compounds have multiple hydroxyl groups reacting with the epoxy network leading to an only slight widening of the network, as it is a network former itself. However, SCP-DOPO-HQ has only one hydroxyl group, so there is no possible continuation of the network, and the network density is decreased. This explains why the polymeric structure of the novolak based structures has less influence on the glass transition temperature. For further work, a stoichiometric adjustment of hardener (hardener in RTM6 plus flame retardant reacting into the network) and TGMDA in the epoxy matrix is still possible to reach even higher glass transition temperatures by adding extra TGMDA to the formulation of the one part epoxy resin RTM6 and the reactive flame retardant.

Table 3: Glass transition temperatures and moisture uptake of RTM6 samples

Sample	T_g (DSC, center)/°C	Moisture uptake/%
RTM6	215	2
+ 10% Novolak-SCP	197	2
+ 10% Novolak-SCP-DOPO	190	2
+ 10% SCP-DOPO-HQ	175	3

Different samples were stored at 70°C in water for 14 days to measure the moisture uptake (see Table 3). There is no significant change in moisture uptake for the examined samples (2–3%) in comparison to neat RTM6 samples (2%). Only SCP-DOPO-HQ with the already discussed lowest network density shows an increase to 3%. Glass transition temperatures of the wet samples show no difference compared to the dry samples because drying occurs before the glass transition temperature is reached.

Table 4 shows interlaminar shear strength (ILSS) of the investigated CFRP samples. The values are additionally normalized to RTM6 samples without flame retardants. The incorporation of 10% Novolak-SCP-DOPO leads to a slight reduction of ILSS of 12%, which is however not significant within the measurement tolerance of the testing method (± 10%). In addition, Novolak-SCP shows an acceptable decrease of 21%. For both, an adjustment of hardening and epoxy component stoichiometry can still be performed to increase these values. Nevertheless, the application of these flame retardants in epoxy-based composites is possible with respect to mechanical performance. The formerly discussed lowering of the network density for SCP-DOPO-HQ shows a higher decrease of ILSS by 28%.

Table 4: ILSS of selected CFRP samples additionally normalized to RTM6 + CF

Sample	ILS/N·mm^{-2}	Relative ILSS/ %
RTM6 + CF	68 ± 3	100 ± 5
+ 10% Novolak-SCP	54 ± 2	79 ± 3
+ 10% Novolak-SCP-DOPO	60 ± 2	88 ± 3
+ 10% SCP-DOPO-HQ	50 ± 3	72 ± 6

3.2.2 Thermal Stability of Neat Resin RTM6 Samples

In order to characterize thermal properties of neat RTM6 samples, thermogravimetric analyses were carried out in synthetic air and nitrogen (see Fig. 7). In nitrogen, typically a one-step mass loss is observed, whereas in synthetic air two steps occur. Flame retarded samples show lower temperatures for the beginning of the decomposition than pure RTM6. Therefore, the incorporated flame retardants act before the matrix decomposes, what is crucial for their high efficiency, especially when acting in the gas phase. Accordingly, initial degradation temperatures corresponding to 1% and 5% mass loss ($T_{1\%}$, $T_{5\%}$) are higher for the pure resin sample, whereas the residues at 800°C are higher for the flame retarded samples, as summarized in Table 5. SCP-DOPO-HQ lowers the $T_{5\%}$ the most by almost 60°C. Novolak containing flame retardants show less impact on the thermal stability but still a decrease by 30°C for Novolak-SCP and 42°C for Novolak-SCP-DOPO. The temperature at the maximum of the mass loss rate (T_{max}) is not significantly changed in comparison to neat RTM6 resin. The residue is increased by almost 10% for each flame retardant indicating a possible action in the condensed phase. According to the epoxy resin decomposition model of Rose and co-workers [70,71], in the temperature range of 300°C to 450°C the decomposition step to stable char and different volatile species takes place. At temperatures above 450°C, the stable char degrades in a further decomposition step. Therefore, the residue at the inflection point between these two decomposition steps is determined as well. The temperature and the residue at this point are both higher for the tested phosphorus-containing specimens indicating a possible condensed phase mechanism. The char of the sample with SCP-DOPO-HQ is less stable (T_{max} 528°C) than char of the other samples, indicating a positive influence by the novolak substructure.

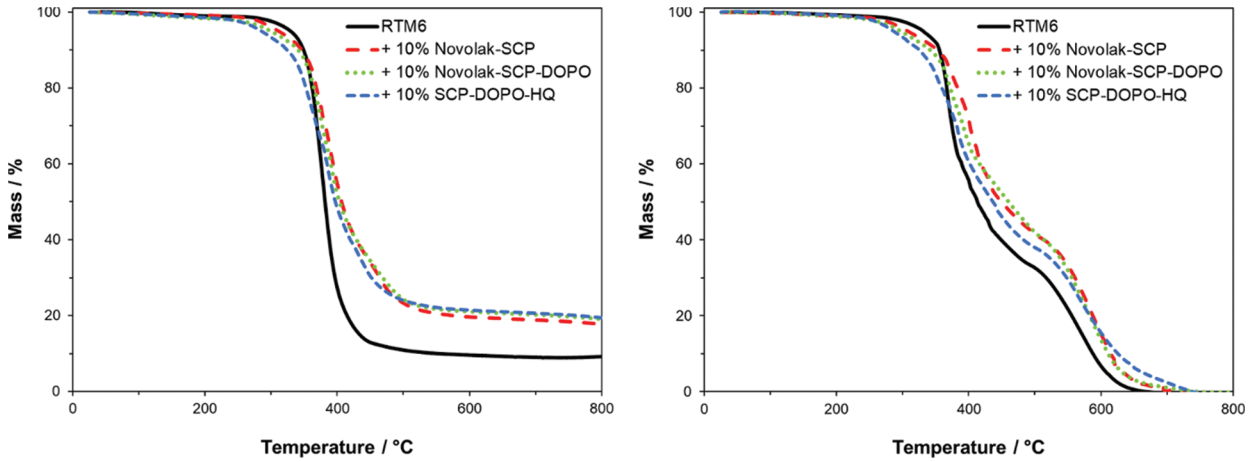

Figure 7: TG-curves of RTM6 and flame retarded samples measured in nitrogen atmosphere (left) and synthetic air (right)

Table 5: T_{max}, $T_{1\%}$, $T_{5\%}$ and residue of formulations of RTM6 and SCP-based flame retardants obtained by TG measurements in air or nitrogen flow (50 mL·min^{-1}) with a heating rate of 10 K·min^{-1}

Sample	T_{max}/°C	$T_{1\%}$/°C	$T_{5\%}$/°C	Residue/%
RTM6, N_2	379	265	341	10
+ 10% Novolak-SCP	376	224	311	18
+ 10% Novolak-SCP-DOPO	393	165	299	19
+ 10% SCP-DOPO-HQ	382	151	285	19
RTM6, air	I 369 | II 572	229	331	33 (492°C) | 0 (800°C)
+ 10% Novolak-SCP	I 402 | II 589	204	308	40 (510°C) | 0 (800°C)
+ 10% Novolak-SCP-DOPO	I 400 | II 570	188	297	39 (521°C) | 0 (800°C)
+ 10% SCP-DOPO-HQ	I 383 | II 528	215	286	37 (508°C) | 0 (800°C)

3.2.3 Flame Retardant Performance

Vertical UL94 tests were carried out to observe the flame spread and flammability of neat resin samples with different contents of flame retardant and a thickness of 4 mm. The results of these tests are summarized in Table 6. RTM6 resin without flame retardant does not reach a classification, the sample burns completely and the burning includes dripping with flames. All flame retarded samples show V-0 classifications for flame retardant contents of 15% but only Novolak-SCP-DOPO shows V-0-classification for a content of 10%. Novolak-SCP-DOPO is the flame retardant with the highest residue in TG measurements of the pure flame retardants. The 10% SCP-DOPO-HQ formulation failed V0 classification only by 4 s regarding the total burning time (5 samples and a total of 10 flame applications). Interestingly, an increase from 10% to 15% Novolak-SCP has a huge impact on the total burning time, since it is decreased from 270 to 19 s. This shows that 10% Novolak-SCP is not sufficient for the formation of a protective barrier and that Novolak-SCP-DOPO acts differently and the both contained phosphorus species act most likely synergistic.

Table 6: UL94-test ratings of RTM6 samples with different flame retardant contents and burning times: average burning times after first and second flame application $t_{av,1st}$ and $t_{av,2nd}$ as well as the total burning time for a series of five samples with a total of ten flame applications $t_{sum5samples}$. NR: not rated

Sample	UL94-rating ($t_{av,1st}$, $t_{av,2nd}$, $t_{sum5samples}$)		
RTM6	**NR** (>60 s)		
Flame retardant content	***7.5%***	***10%***	***15%***
+ Novolak-SCP	**NR** (> 60 s)	**NR** (53.9 s, 0 s, 270 s)	**V-0** (3.2 s, 0.5 s, 19 s)
+ Novolak-SCP-DOPO	**V-1** (2.8 s, 14.4 s, 86 s)	**V-0** (3.9 s, 1.6 s, 28 s)	—
+ SCP-DOPO-HQ	—	**V-1** (3.5 s, 7.2 s, 54 s)	**V-0** (2.2 s, 0.9 s, 16 s)

Additionally, it has to be mentioned, that Novolak-SCP-DOPO has the lowest phosphorus content (6%) compared to Novolak-SCP (8%) and SCP-DOPO-HQ (12%), leading to a phosphorus content of only 0.6% in a 10% formulation with RTM6. This is supporting the observation of a very high flame retardant efficiency of Novolak-SCP-DOPO. Therefore, the varying phosphorus content of the different flame retardants plays a minor role for these investigations.

To investigate the burning behavior under forced conditions, neat resin samples (thickness 4 mm) were tested in a cone calorimeter at a heat flux of 35 $kW \cdot m^{-2}$. Composite materials (thickness 2 mm) were investigated at a heat flux of 60 $kW \cdot m^{-2}$ instead, to quantify a possible fiber degradation. This heat flux and an irradiation time of 20 min led to a carbon fiber degradation, which is expected to occur in burning events like a kerosene fire. The HRR (heat release rate) in dependence on time is presented in Fig. 8. Values of important parameters including time to ignition (tti), peak of heat release rate (pHRR), total heat release (THR), maximum average rate of heat emission (MARHE) and the total smoke release (TSR) are summarized in Table 7. MARHE is an established parameter in cone calorimetry analysis that describes the velocity of the burning. For 2 mm thick reinforced samples, the sum parameters were determined after 300 s of testing and for 4 mm neat resin samples after 500 s. Hand lay-up leads to slight differences in the fiber to volume ratio. This is considered by the value X as the ratio of the combustible material mass (equal to the mass of the matrix and flame retardant) to the whole sample mass. It is also included in the table and used to determine comparable sum parameters THR and TSR.

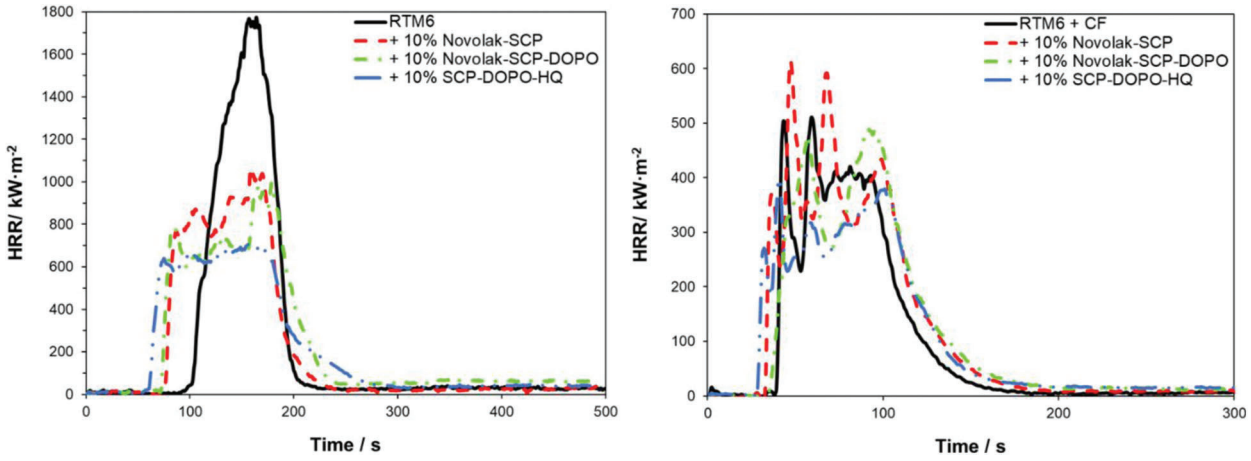

Figure 8: HRR of non-reinforced samples at 35 $kW \cdot m^{-2}$ (left) and of reinforced samples at 60 $kW \cdot m^{-2}$ (right)

Table 7: Results of cone calorimetry (neat resin RTM6 + flame retardant: sample thickness 4 mm, composites (RTM6 + flame retardant + CF): sample thickness 2 mm)

Sample	tti/s	pHRR/ $kW \cdot m^{-2}$	THR·X^{-1}/ $MJ \cdot m^{-2}$	MARHE/ $kW \cdot m^{-2}$	TSR·X^{-1}/ $m^2 \cdot m^{-2}$	THR·ML^{-1}/ $kW \cdot m^{-2} \cdot g^{-1}$	Residue/%	X
RTM6	94 ± 1	1715 ± 58	104 ± 1	550 ± 6	5601 ± 31	2.3	4 ± 2	1
+ 10% Novolak-SCP	72 ± 7	1071 ± 39	101 ± 1	476 ± 17	5216 ± 125	2.2	17 ± 1	1
+ 10% Novolak-SCP-DOPO	70 ± 4	1000 ± 12	105 ± 3	455 ± 9	5451 ± 173	2.2	18 ± 2	1
+ 10% SCP-DOPO-HQ	58 ± 3	781 ± 74	102 ± 1	434 ± 11	5059 ± 5	2.2	19 ± 1	1
RTM6 + CF	31 ± 2	492 ± 19	72 ± 1	242 ± 5	3763 ± 165	2.5	59 ± 1	0.43
+ 10% Novolak-SCP	29 ± 1	552 ± 10	75 ± 3	269 ± 9	3778 ± 96	2.5	57 ± 1	0.46
+ 10% Novolak-SCP-DOPO	30 ± 2	514 ± 17	66 ± 3	256 ± 8	3689 ± 179	1.9	58 ± 2	0.49
+ 10% SCP-DOPO-HQ	26 ± 3	372 ± 19	63 ± 4	221 ± 13	3641 ± 221	1.9	58± 2	0.50

Note: X: ratio of the combustible material mass (resin + flame retardant) to the whole sample mass.

Neat RTM6 burns rapidly and continuously resulting in a sharp HRR peak. RTM6 samples containing flame retardants show broader and lower, plateau-like peaks in HRR, while THR is not influenced, indicating a charring mechanism in the condensed phase and formation of a barrier [67]. pHRR, MARHE and TSR are decreased for flame retarded formulations. Especially pHRR is decreased by up to 54% for SCP-DOPO-HQ and up to 42% for novolak containing samples. The addition of these flame retardants decreases the tti. Total Heat Release per Mass Loss (THR·ML^{-1}) provides information on flame retardant mechanisms since referring to evolved heat per mass of volatiles [2]. A lower value in comparison to the non-flame retarded sample (2.3 $kW \cdot m^{-2} \cdot g^{-1}$) is connected to more gas phase activity of a flame retardant. Therefore, all flame retardants act mainly in the condensed phase because THR·ML^{-1} is almost the same for every sample, which is also indicated by the shape of the HRR curves. Additionally, TSR is decreased by the incorporation of flame retardants and the residues are higher for all flame retarded samples than for the neat resin (4%). It is highest for SPC-DOPO-HQ that also showed the highest reduction of pHRR and has the highest phosphorus content (1.2% in a 10% formulation with RTM6). Therefore, the forced burning conditions of cone calorimetric analysis indicate other flame retardant efficiencies and mechanisms than UL94 tests.

The incorporation of a fiber reinforcement leads to other shapes in HRR curves. Sharp peaks represent delamination processes. Single plies separate and burn fast and fierce since gas between the fiber plies acts as a heat barrier. Due to the high heat flux (60 $kW \cdot m^{-2}$) required for fiber degradation, the standard deviation rises. All sum parameters are lower for reinforced samples in comparison to neat resin samples because of the smaller amounts of combustible material. Due to the higher heat flux and the high surface to volume ratio in the composite material, char formation is less effective. For DOPO containing flame retardants, the THR is decreased by up to 9% and pHRR is decreased by up to 24% for SCP-DOPO-HQ. More differences cannot be detected, as the heat flux is very high, and these very harsh conditions are critical for the flame retardant action. This is also shown by TSR values, since they only differ within the error range. Nevertheless, according to the value of THR·ML^{-1}, Novolak-SCP-DOPO and SCP-DOPO-HQ act in the gas phase (1.9 $kW \cdot m^{-2} \cdot g^{-1}$) in comparison to non-flame retarded samples or Novolak-SCP (2.5 $kW \cdot m^{-2} \cdot g^{-1}$). This shows that the flame retardant mode of action is dependent on fiber reinforcement as Novolak-SCP-DOPO and SCP-DOPO-HQ act differently in reinforced and non-reinforced samples. Finally, the residue corrected by the fiber content in the samples is also highest for Novolak-SCP-DOPO (7%) and SCP-DOPO-HQ (8%) in comparison to RTM6 (2%) or Novolak-SCP (3%) showing a simultaneous mode of action in gas and condensed phase for the DOPO containing flame retardants.

3.2.4 Residue of Neat Resin Samples

Fig. 9 shows SEM images of the residues obtained after cone calorimetry at 35 kW·m^{-2} for 10 min. While RTM6 alone (A) forms a highly instable residue that contains small holes (diameter about 50–100 µm), the addition of phosphorus containing flame retardants (B,C,D) leads to residues that are more stable and have a closed structure and therefore residues that are a better protection from heat or oxygen. DOPO containing flame retardants (B, D) additionally show a microstructure on the surface indicating another decomposition mechanism of the flame retarded matrix.

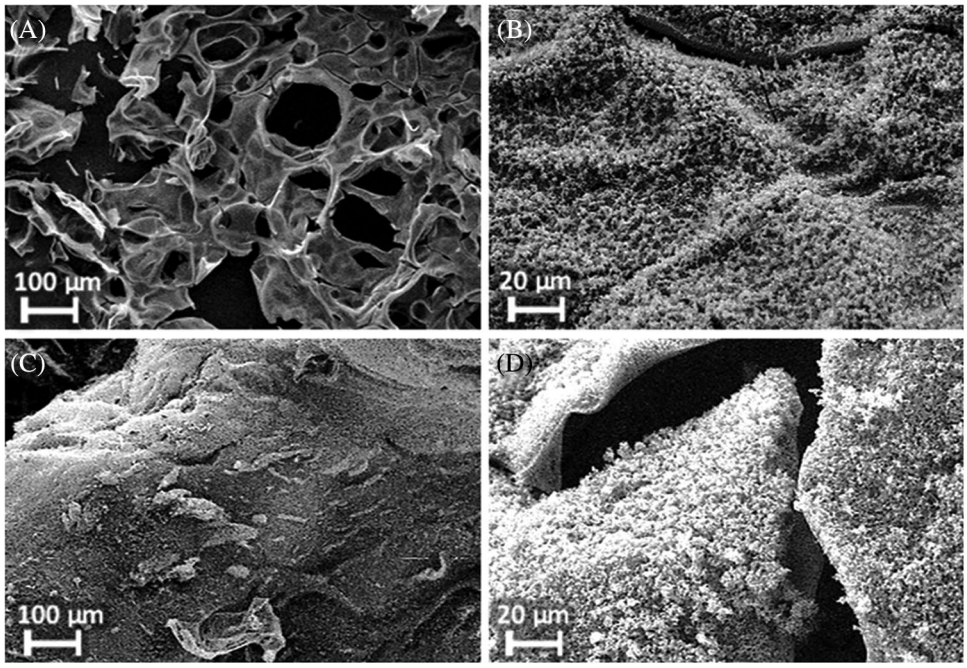

Figure 9: SEM images of residues after irradiation of neat resin samples at 35 kW·m^{-2} for 10 min: (A): RTM6, (B): RTM6 + 10% SCP-DOPO-HQ, (C): RTM6 + 10% Novolak-SCP, (D): RTM6 + 10% Novolak-SCP-DOPO

3.2.5 Fiber Protection Efficiency

The fiber residues of the reinforced samples after 20 min at 60 kW·m^{-2} in cone calorimetry were investigated by SEM and EDX to determine if there is a fiber protection and to get a mechanistic insight. SEM images of at least 30 single fibers were used to determine a mean fiber diameter. Mean fiber diameters and the smallest diameter that has been measured are summarized in Table 8. The diameter of untreated carbon fibers is (7.3 ± 0.2) µm. While pure RTM6 matrix leads to an amount of carbon fiber fragments with critical diameters below 3 µm (3.3 ± 0.7 µm, smallest diameter: 2.1 µm) according to the WHO-definition, all flame retarded samples prevent the formation of respirable carbon fibers. Especially Novolak-SCP and SCP-DOPO-HQ show higher mean fiber diameters of (6.0 ± 0.7) µm after irradiation. Nevertheless, Novolak-SCP-DOPO shows a lower standard deviation of its mean fiber diameter (5.2 ± 0.4 µm) as well as a higher smallest diameter with 4.4 µm in comparison to Novolak-SCP with 4.1 µm. The smallest diameter is crucial as no respirable fiber fragments should be released into the environment. The observations lead to the conclusion, that mixed phosphorus species like the mixture of SCP and DOPO induce a better and more even protection of the fibers.

Table 8: Mean diameter, standard deviation and smallest measured diameter of at least 30 carbon fibers in composite materials with partially flame retarded RTM6 after irradiation at 60 $kW \cdot m^{-2}$ for 20 min determined by SEM

Sample	Mean diameter/µm	Smallest diameter/µm
RTM6 + CF	3.3 ± 0.7	2.1
+ 10% Novolak-SCP	6.0 ± 0.7	4.1
+ 10% Novolak-SCP-DOPO	5.2 ± 0.4	4.4
+ 10% SCP-DOPO-HQ	6.0 ± 0.6	4.7

To get a better understanding of the fiber protection, EDX measurements were carried out. A mapping for the composite sample residue with 10% Novolak-SCP-DOPO in the matrix is shown in Fig. 10. It can be seen, that phosphorus and oxygen belong together as residue of the flame retardant as well as carbon and nitrogen as residual fiber. This shows the formation of typical phosphoric acid like structures during combustion. Since EDX not only measures the surface but also a certain depth, these mapping images do not show, if there is phosphorus continuously found on the fiber surface. Because of that, molar element concentrations on different spots were determined. Fig. 11 shows the choice of spots, in which the first spot (X1) is an agglomerate that is visible on the surface and the second spot (X2) has no visible residue. The element concentrations are summarized in Table 9. Every measured spot contains phosphorus but in different amounts. The ratios of phosphorus to oxygen range from mostly 1:2 to 1:4, so in between the chemical structure of phosphate glass, polyphosphoric acid that is a typical reaction product for condensed phase mechanisms and single phosphates. Especially agglomerates show a ratio 1:2/1:3, whereas, the ratio is more likely 1:4 on the direct fiber surface. This is consistent to observations made for the protection of graphite from oxidation by impregnation with organic phosphate and phosphite esters in literature [72]. The authors assume a covalent bonding on the graphite surface in form of C-OPO_3 groups leading to a hydrophilic surface. Graphite and carbon fibers have similar chemical structures, so directly on the fiber surface similar reactions may occur and lead to the ratio of phosphorus to oxygen from 1:4. The continuous observation of phosphorus species on the fiber surface shows the mechanism of fiber protection as apparently these residues hinder the oxidation of the carbon fibers efficiently.

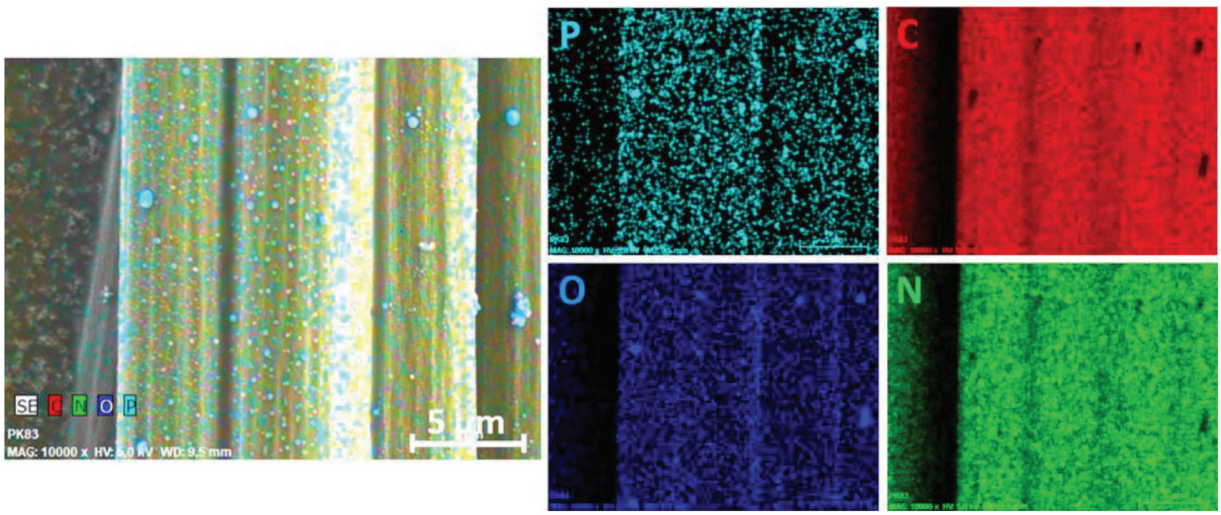

Figure 10: EDX mapping results for RTM6 + CF + Novolak-SCP-DOPO (fiber residues) after irradiation at 60 $kW \cdot m^{-2}$ for 20 min

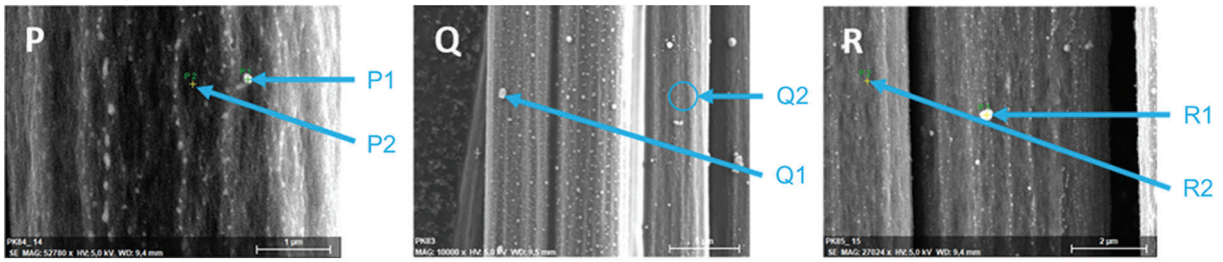

Figure 11: SEM images of carbon fibers after irradiation at 60 $kW \cdot m^{-2}$ for 20 min: P: RTM6 + CF + Novolak-SCP, Q: RTM6 + CF + 10% Novolak-SCP-DOPO and R: RTM6 + CF + 10% SCP-DOPO-HQ

Table 9: Molar element concentrations on different spots (see Fig. 11) of fiber residues after irradiation (60 $kW \cdot m^{-2}$ for 20 min)

EDX-spectra of fiber residue	C/%	N/%	O/%	P/%
RTM6 + 10% Novolak-SCP				
P1	80.1	4.2	10.6	4.3
P2	92.0	3.8	3.6	0.5
RTM6 + 10% Novolak-SCP-DOPO				
Q1	82.6	3.8	9.6	2.7
Q2	89.4	4.4	4.8	1.1
RTM6 + 10% SCP-DOPO-HQ				
R1	50.2	2.8	28.4	13.9
R2	91.1	2.1	5.5	1.2

4 Conclusions

SCP as biobased phosphorus compound was successfully used to synthesize new flame retardants with novolak or DOPO-HQ. The advantages of SCP are on first sight its high phosphorus and aromatic content as well as its high reactivity and easy conversion with for example hydroxyl groups. The results proof the processability of the synthesized reactive, soluble and partially polymeric flame retardants with an epoxy resin by resin transfer moulding. Residual hydroxyl groups are incorporated into the epoxy resin network resulting in minor changes in glass transition temperature and interlaminar shear strength for novolak containing flame retardants compared to the resin without flame retardants. SCP-DOPO-HQ with one residual hydroxyl group per molecule lowers the network density pronouncedly and leads to a higher decrease. A synergism in char formation is observed if both, SCP and DOPO, are present in the flame retardant. UL94 V0-classifications are reached with 10% Novolak-SCP-DOPO, 15% Novolak-SCP or 15% SCP-DOPO-HQ in neat resin samples. Cone calorimetric measurements of neat resin formulations with 10% flame retardant show a reduction of peak of heat release rate by up to 54% compared to the unmodified epoxy resin. The amount of residue is four to five times increased. The mode of action is dependent on the reinforcement of the samples. In non-reinforced samples, DOPO containing and not containing flame retardants act alike, whereas in reinforced samples, gas phase activity is mainly observed for DOPO-containing flame retardants. Due to a large matrix surface, gas phase activity is more efficient in composite materials than activity in the condensed phase. In this case, the mode of action adapts to neat resin or fiber-reinforced samples, so there is efficient flame retardancy in both cases. SEM

images show a stable, continuous char for flame retarded neat resin samples and an effective fiber protection with a phosphorus and oxygen containing protection layer on the fiber surface after combustion.

This research shows the versatility of SCP to synthesize new flame retardants with a high bio-based carbon content and adjusted properties for different problems or applications.

Funding Statement: The authors received no specific funding for this study.

Conflicts of Interest: The authors declare that they have no conflicts of interest to report regarding the present study.

References

1. Dao, D. Q., Rogaume, T., Luche, J., Richard, F., Bustamante, V. et al. (2016). Thermal degradation of epoxy resin/carbon fiber composites: Influence of carbon fiber fraction on the fire reaction properties and on the gaseous species release. *Fire and Materials, 40(1),* 27–47. DOI 10.1002/fam.2265.
2. Perret, B., Schartel, B., Stöß, K., Ciesielski, M., Diederichs, J. et al. (2011). Novel DOPO-based flame retardants in high-performance carbon fibre epoxy composites for aviation. *European Polymer Journal, 47(5),* 1081–1089. DOI 10.1016/j.eurpolymj.2011.02.008.
3. Hume, J. (1992). Assessing the fire performance characteristics of GRP composites. *International Conference on Materials and Design Against Fire,* pp. 11–15. London.
4. Becker, C. M., Dick, T. A., Wypych, F., Schrekker, H. S., Amico, S. C. (2012). Synergetic effect of LDH and glass fiber on the properties of two-and three-component epoxy composites. *Polymer Testing, 31(6),* 741–747. DOI 10.1016/j.polymertesting.2012.04.009.
5. Levchik, S. V., Camino, G., Costa, L., Luda, M. P. (1996). Mechanistic study of thermal behaviour and combustion performance of carbon fibre-epoxy resin composites fire retarded with a phosphorous-based curing system. *Polymer Degradation and Stability, 54(2–3),* 317–322. DOI 10.1016/S0141-3910(96)00057-2.
6. Martin, F. J., Price, K. R. (1968). Flammability of epoxy resins. *Journal of Applied Polymer Science, 12(1),* 143–158. DOI 10.1002/app.1968.070120114.
7. Toldy, A., Szolnoki, B., Marosi, G. (2011). Flame retardancy of fibre-reinforced epoxy resin composites for aerospace applications. *Polymer Degradation and Stability, 96(3),* 371–376. DOI 10.1016/j.polymdegradstab.2010.03.021.
8. Rabe, S., Chuenban, Y., Schartel, B. (2017). Exploring the modes of action of phosphorus-based flame retardants in polymeric systems. *Materials, 10(5),* 455. DOI 10.3390/ma10050455.
9. Lewin, M., Weil, E. D. (2001). Mechanisms and modes of action in flame retardancy of polymers. In: Horrocks, A. R., Price, D. (Eds.), *Fire retardant materials,* pp. 31–68. UK: Woodhead Publishing Limited.
10. Schartel, B. (2010). Phosphorus-based flame retardancy mechanisms-old hat or a starting point for future development? *Materials, 3(10),* 4710–4745. DOI 10.3390/ma3104710.
11. Lorenzetti, A., Modesti, M., Besco, S., Hrelja, D., Donadi, S. (2011). Influence of phosphorus valency on thermal behaviour of flame retarded polyurethane foams. *Polymer Degradation and Stability, 96(8),* 1455–1461. DOI 10.1016/j.polymdegradstab.2011.05.012.
12. Pawlowski, K. H., Schartel, B. (2007). Flame retardancy mechanisms of triphenyl phosphate, resorcinol bis (diphenyl phosphate) and bisphenol A bis (diphenyl phosphate) in polycarbonate/acrylonitrile–butadiene–styrene blends. *Polymer International, 56(11),* 1404–1414. DOI 10.1002/(ISSN)1097-0126.
13. Lai, X., Zeng, X., Li, H., Liao, F., Yin, C. et al. (2012). Synergistic effect of phosphorus-containing montmorillonite with intumescent flame retardant in polypropylene. *Journal of Macromolecular Science, Part B, 51(6),* 1186–1198. DOI 10.1080/00222348.2011.625909.
14. Buck, K. T., Boeing, A. J., Dolfini, J. E. (1987). Method of producing benzaldehyde. U.S. Patent US4673766.
15. Bourbigot, S., Le Bras, M., Delobel, R. (1993). Carbonization mechanisms resulting from intumescence association with the ammonium polyphosphate-pentaerythritol fire retardant system. *Carbon, 31(8),* 1219–1230. DOI 10.1016/0008-6223(93)90079-P.

16. Wang, Z., Lv, P., Hu, Y., Hu, K. (2009). Thermal degradation study of intumescent flame retardants by TG and FTIR: Melamine phosphate and its mixture with pentaerythritol. *Journal of Analytical and Applied Pyrolysis, 86(1),* 207–214. DOI 10.1016/j.jaap.2009.06.007.
17. Zhang, T., Yan, H., Shen, L., Fang, Z., Zhang, X. et al. (2014). Chitosan/Phytic acid polyelectrolyte complex: A green and renewable intumescent flame retardant system for ethylene–Vinyl acetate copolymer. *Industrial & Engineering Chemistry Research, 53(49),* 19199–19207. DOI 10.1021/ie503421f.
18. Lolas, G. M., Markakis, P. (1975). Phytic acid and other phosphorus compounds of beans (*Phaseolus vulgaris* L.). *Journal of Agricultural and Food Chemistry, 23(1),* 13–15. DOI 10.1021/jf60197a016.
19. Wang, P. J., Liao, D. J., Hu, X. P., Pan, N., Li, W. X. et al. (2019). Facile fabrication of biobased P N C-containing nano-layered hybrid: Preparation, growth mechanism and its efficient fire retardancy in epoxy. *Polymer Degradation and Stability, 159,* 153–162. DOI 10.1016/j.polymdegradstab.2018.11.024.
20. Howell, B. A., Carter, K. E., Dangalle, H. (2011). Flame retardants based on tartaric acid: A renewable by-product of the wine industry. In: *Renewable and sustainable polymers,* pp. 133–152. USA: American Chemical Society.
21. Prieur, B., Meub, M., Wittemann, M., Klein, R., Bellayer, S. et al. (2017). Phosphorylation of lignin: Characterization and investigation of the thermal decomposition. *RSC Advances, 7(27),* 16866–16877. DOI 10.1039/C7RA00295E.
22. Yang, H., Yu, B., Xu, X., Bourbigot, S., Wang, H. et al. (2020). Lignin-derived bio-based flame retardants toward high-performance sustainable polymeric materials. *Green Chemistry, 22(7),* 2129–2161. DOI 10.1039/D0GC00449A.
23. Jin, S., Qian, L., Qiu, Y., Chen, Y., Xin, F. (2019). High-efficiency flame retardant behavior of bi-DOPO compound with hydroxyl group on epoxy resin. *Polymer Degradation and Stability, 166,* 344–352. DOI 10.1016/j.polymdegradstab.2019.06.024.
24. Howell, B. A., Sun, W. (2018). Biobased flame retardants from tartaric acid and derivatives. *Polymer Degradation and Stability, 157,* 199–211. DOI 10.1016/j.polymdegradstab.2018.10.006.
25. Ma, S., Liu, X., Jiang, Y., Fan, L., Feng, J. et al. (2014). Synthesis and properties of phosphorus-containing bio-based epoxy resin from itaconic acid. *Science China Chemistry, 57(3),* 379–388. DOI 10.1007/s11426-013-5025-3.
26. Ecochard, Y., DeCostanzi, M., Negrell, C., Sonnier, R., Caillol, S. (2019). Cardanol and eugenol based flame retardant epoxy monomers for thermostable networks. *Molecules, 24(9),* 1818. DOI 10.3390/molecules24091818.
27. Abell, J. P., Yamamoto, H. (2008). Catalytic enantioselective pudovik reaction of aldehydes and aldimines with tethered bis (8-quinolinato) (TBOx) aluminum complex. *Journal of the American Chemical Society, 130(32),* 10521–10523. DOI 10.1021/ja803859p.
28. Xie, C., Zeng, B., Gao, H., Xu, Y., Luo, W. et al. (2014). Improving thermal and flame-retardant properties of epoxy resins by a novel reactive phosphorous-containing curing agent. *Polymer Engineering & Science, 54(5),* 1192–1200. DOI 10.1002/pen.23642.
29. Liu, J., Dai, J., Wang, S., Peng, Y., Cao, L. et al. (2020). Facile synthesis of bio-based reactive flame retardant from vanillin and guaiacol for epoxy resin. *Composites Part B: Engineering, 190,* 107926. DOI 10.1016/j.compositesb.2020.107926.
30. Howell, B. A., Daniel, Y. G. (2020). Reactive flame retardants from starch-derived isosorbide. In: *Sustainability & green polymer chemistry,* vol. 1, pp. 209–219. USA: American Chemical Society.
31. Howell, B. A., Han, X. (2020). Effective biobased phosphorus flame retardants from starch-derived bis-2, 5-(hydroxymethyl) furan. *Molecules, 25(3),* 592. DOI 10.3390/molecules25030592.
32. Guo, J., Song, H., Liu, H., Luo, C., Ren, Y. et al. (2017). Polypyrrole-interface-functionalized nano-magnetite epoxy nanocomposites as electromagnetic wave absorbers with enhanced flame retardancy. *Journal of Materials Chemistry C, 5(22),* 5334–5344. DOI 10.1039/C7TC01502J.
33. Hussain, M., Varley, R. J., Mathys, Z., Cheng, Y. B., Simon, G. P. (2004). Effect of organo-phosphorus and nano-clay materials on the thermal and fire performance of epoxy resins. *Journal of Applied Polymer Science, 91(2),* 1233–1253. DOI 10.1002/(ISSN)1097-4628.
34. Zhang, X., He, Q., Gu, H., Colorado, H. A., Wei, S. et al. (2013). Flame-retardant electrical conductive nanopolymers based on bisphenol F epoxy resin reinforced with nano polyanilines. *ACS Applied Materials & Interfaces, 5(3),* 898–910. DOI 10.1021/am302563w.

35. Kalali, E. N., Wang, X. (2015). Functionalized layered double hydroxide-based epoxy nanocomposites with improved flame retardancy and mechanical properties. *Journal of Materials Chemistry A, 3(13),* 6819–6826. DOI 10.1039/C5TA00010F.
36. Wang, H., Li, S., Zhu, Z., Yin, X., Wang, L. et al. (2021). A novel DOPO-based flame retardant containing benzimidazolone structure with high charring ability towards low flammability and smoke epoxy resins. *Polymer Degradation and Stability, 183,* 109426. DOI 10.1016/j.polymdegradstab.2020.109426.
37. Qian, L. J., Ye, L. J., Xu, G. Z., Liu, J., Guo, J. Q. (2011). The non-halogen flame retardant epoxy resin based on a novel compound with phosphaphenanthrene and cyclotriphosphazene double functional groups. *Polymer Degradation and Stability, 96(6),* 1118–1124. DOI 10.1016/j.polymdegradstab.2011.03.001.
38. Gao, L. P., Wang, D. Y., Wang, Y. Z., Wang, J. S., Yang, B. (2008). A Flame-retardant epoxy resin based on a reactive phosphorus-containing monomer of DODPP and its thermal and flame-retardant properties. *Polymer Degradation and Stability, 93(7),* 1308–1315. DOI 10.1016/j.polymdegradstab.2008.04.004.
39. Wang, H., Yuan, J., Zhu, Z., Yin, X., Weng, Y. et al. (2021). High performance epoxy resin composites modified with multifunctional thiophene/phosphaphenanthrene-based flame retardant: Excellent flame retardance, strong mechanical property and high transparency. *Composites Part B: Engineering, 227,* 109392. DOI 10.1016/j.compositesb.2021.109392.
40. Zhu, Z., Lin, P., Wang, H., Wang, L., Yu, B. et al. (2020). A facile one-step synthesis of highly efficient melamine salt reactive flame retardant for epoxy resin. *Journal of Materials Science, 55(27),* 12836–12847. DOI 10.1007/s10853-020-04935-6.
41. Zhu, Z. M., Wang, L. X., Lin, X. B., Dong, L. P. (2019). Synthesis of a novel phosphorus-nitrogen flame retardant and its application in epoxy resin. *Polymer Degradation and Stability, 169,* 108981. DOI 10.1016/j.polymdegradstab.2019.108981.
42. Gu, J., Dang, J., Wu, Y., Xie, C., Han, Y. (2012). Flame-retardant, thermal, mechanical and dielectric properties of structural non-halogenated epoxy resin composites. *Polymer-Plastics Technology and Engineering, 51(12),* 1198–1203. DOI 10.1080/03602559.2012.694951.
43. Toldy, A., Szolnoki, B., Csontos, I., Marosi, G. (2014). Green synthesis and characterization of phosphorus flame retardant crosslinking agents for epoxy resins. *Journal of Applied Polymer Science, 131(7),* 40105. DOI 10.1002/app.40105.
44. Ménard, R., Negrell, C., Fache, M., Ferry, L., Sonnier, R. et al. (2015). From a bio-based phosphorus-containing epoxy monomer to fully bio-based flame-retardant thermosets. *RSC Advances, 5(87),* 70856–70867. DOI 10.1039/C5RA12859E.
45. Ménard, R., Negrell, C., Ferry, L., Sonnier, R., David, G. (2015). Synthesis of biobased phosphorus-containing flame retardants for epoxy thermosets comparison of additive and reactive approaches. *Polymer Degradation and Stability, 120,* 300–312. DOI 10.1016/j.polymdegradstab.2015.07.015.
46. Chvertkina, L. V., Khoklov, P. S., Mironov, V. F. (1992). Phosphorus dericatives of salicylic acid. *Russian Chemical Reviews, 61(10),* 1009. DOI 10.1070/RC1992v061n10ABEH001013.
47. Young, R. W. (1952). A Re-examination of the reaction between phosphorus trichloride and salicylic acid. *Journal of the American Chemical Society, 74(7),* 1672–1673. DOI 10.1021/ja01127a017.
48. Hedner, T., Everts, B. (1998). The early clinical history of salicylates in rheumatology and pain. *Clinical Rheumatology, 17(1),* 17–25. DOI 10.1007/BF01450953.
49. Mahdi, J. G., Mahdi, A. J., Mahdi, A. J., Bowen, I. D. (2006). The historical analysis of aspirin discovery, its relation to the willow tree and antiproliferative and anticancer potential. *Cell Proliferation, 39(2),* 147–155. DOI 10.1111/j.1365-2184.2006.00377.x.
50. Wang, X., Hu, Y., Song, L., Xing, W., Lu, H. et al. (2010). Flame retardancy and thermal degradation mechanism of epoxy resin composites based on a DOPO substituted organophosphorus oligomer. *Polymer, 51(11),* 2435–2445. DOI 10.1016/j.polymer.2010.03.053.
51. Moy, P. Y., Gregor, A. I., Pirelli, R. L., Bright, D. A. (2009). Oligomeric Bis-phosphate flame retardants and compositions containing the same. EP2089402 B1.

52. Hamciuc, C., Vlad-Bubulac, T., Serbezeanu, D., Carja, I. D., Hamciuc, E. et al. (2016). Environmentally friendly fire-resistant epoxy resins based on a new oligophosphonate with high flame retardant efficiency. *RSC Advances, 6(27),* 22764–22776. DOI 10.1039/C5RA27451F.
53. Wang, X., Hu, Y., Song, L., Yang, H., Xing, W. et al. (2011). Synthesis and characterization of a DOPO-substitued organophosphorus oligomer and its application in flame retardant epoxy resins. *Progress in Organic Coatings, 71(1),* 72–82. DOI 10.1016/j.porgcoat.2010.12.013.
54. Greiner, L., Kukla, P., Eibl, S., Döring, M. (2019). Phosphorus containing polyacrylamides as flame retardants for epoxy-based composites in aviation. *Polymers, 11(2),* 284. DOI 10.3390/polym11020284.
55. Iji, M., Kiuchi, Y. (2001). Flame-retardant epoxy resin compounds containing novolac derivatives with aromatic compounds. *Polymers for Advanced Technologies, 12(7),* 393–406. DOI 10.1002/(ISSN)1099-1581.
56. Minegishi, S., Komatsu, S., Kameyama, A., Nishikubo, T. (1999). Novel synthesis of polyphosphonates by the polyaddition of bis (epoxide) with diaryl phosphonates. *Journal of Polymer Science Part A: Polymer Chemistry, 37(7),* 959–965. DOI 10.1002/(ISSN)1099-0518.
57. Eibl, S. (2017). Potential for the formation of respirable fibers in carbon fiber reinforced plastic materials after combustion. *Fire and Materials, 41,* 808–816. DOI 10.1002/fam.2423.
58. Hertzberg, T., Blomqvist, P. (2003). Particles from fires—A screening of common materials found in buildings. *Fire and Materials, 27(6),* 295–314. DOI 10.1002/fam.837.
59. Hertzberg, T. (2005). Dangers relating to fires in carbon-fibre based composite material. *Fire and Materials, 29(4),* 231–248. DOI 10.1002/fam.882.
60. Holt, P. F., Horne, M. (1978). Dust from carbon fibre. *Environmental Research, 17(2),* 276–283. DOI 10.1016/0013-9351(78)90030-0.
61. World Health Organization (1999). Hazard prevention and control in the work environment: Airborne dust. WHO/SDE/OEH/99.14. http://www.who.int/occupational_health/publications/en/oehairbornedust3.pdf.
62. Greiner, L., Döring, M., Eibl, S. (2021). Prevention of the formation of respirable fibers in carbon fiber reinforced epoxy resins during combustion by phosphorus or silicon containing flame retardants. *Polymer Degradation and Stability, 185,* 109497. DOI 10.1016/j.polymdegradstab.2021.109497.
63. Hexcel Corporation (2018). Product data sheet HexFlow®RTM6. www.hexcel.com.
64. Deutsches Instutut für Normung e.V. (2015). DIN EN 60695-11-10 Prüfungen zur Beurteilung der Brandgefahr-Teil 11-10: Prüfflammen-Prüfverfahren mit einer 50-W-Prüfflamme horizontal und vertikal (IEC 60695-11-10:2013). Germany.
65. Babrauskas, V. (1984). Development of the cone calorimeter-A bench-scale heat release rate apparatus based on oxygen consumption. *Fire and Materials, 8(2),* 81–95. DOI 10.1002/FAM.810080206.
66. International Organization for Standardization (2015). ISO 5660-1:2015 Reaction-to-fire tests-heat release, smoke production and mass loss rate. Switzerland.
67. Schartel, B., Hull, T. R. (2007). Development of fire-retarded materials—Interpretation of cone calorimeter data. *Fire and Materials, 31(5),* 327–354. DOI 10.1002/fam.949.
68. Deutsches Instutut für Normung e.V. (1997). DIN EN 2563:1997-03 Aerospace series- carbon fiber reinforced plastics- unidirectional laminates; determination of apparent interlaminar shear strength. Germany.
69. He, M., Zhang, D., Zhao, W., Qin, S., Yu, J. (2019). Flame retardant and thermal decomposition mechanism of poly (butylene terephthalate)/DOPO-HQ composites. *Polymer Composites, 40(3),* 974–985. DOI 10.1002/pc.24772.
70. Rose, N., Le Bras, M., Delobel, R., Costes, B., Henry, Y. (1993). Thermal oxidative degradation of an epoxy resin. *Polymer Degradation and Stability, 42(3),* 307–316. DOI 10.1016/0141-3910(93)90226-9.
71. Rose, N., Le Bras, M., Bourbigot, S., Delobel, R. (1994). Thermal oxidative degradation of epoxy resins: Evaluation of their heat resistance using invariant kinetic parameters. *Polymer Degradation and Stability, 45(3),* 387–397. DOI 10.1016/0141-3910(94)90209-7.
72. McKee, D. W., Spiro, C. L., Lamby, E. J. (1984). The inhibition of graphite oxidation by phosphorus additives. *Carbon, 22(3),* 285–290. DOI 10.1016/0008-6223(84)90172-6.